Characterisation of transcriptional and chromatin events in relation to floral transition and identification of nuclear organisation determinants

del Prete, S.

Chapter 4

Early Transcriptional Events Associated with Floral Transition in Arabidopsis Leaves Induced by a Short-day to Long-day Switch

Stefania Del Prete[a,b], Delphine Charif[a], Fabienne Granier[a], Ludivine Taconnat[c], Véronique Brunaud[c], Paul Fransz[b], Valérie Gaudin[a]

Author affiliations

[a]Institut Jean-Pierre Bourgin, INRA, AgroParisTech, CNRS, Université Paris-Saclay, F-78000 Versailles, France

[b]Department of Plant Development and (Epi)Genetics, Swammerdam Institute for Life Sciences, University of Amsterdam, Amsterdam, the Netherlands

[c]Institute of Plant Sciences Paris Saclay IPS2, CNRS, INRA, Université Paris-Sud, Université Evry, Université Paris-Saclay, Bâtiment 630, 91405 Orsay, France.

This chapter is part of a paper in preparation.

Abstract

Flowering time results from a complex interplay between endogenous and environmental cues. The various stimuli are sensed by the different organs, therefore the floral transition is an integrated process that requires the whole plant. Light is one of the important signals triggering flowering time in Arabidopsis and is perceived by leaves. Furthermore, the leaf photosynthetic activity produces important metabolites that participate to a florigen signal. Despite the key role of leaves in this process, our knowledge of the global changes in transcript expression profiles is rather limited. Here, we investigate the early transcriptional events associated with floral transition using a photoperiodic switch to induce flowering initiation. Our genome-wide analysis allowed the identification of a large set of differentially expressed genes at various time points during the transition, highlighting the dynamics of the leaf gene-network and the molecular processes underlying this developmental phase. This analysis provides a list of interesting new candidates involved in the floral transition in mature leaves.

Introduction

The flowering transition is the switch from a vegetative to a reproductive developmental growth responding in a controlled way to various environmental and endogenous cues (McClung et al., 2016; Bratzel and Turck, 2015; Li et al., 2016). It is a plastic phase characterised by transcriptional reprogramming (Srikanth and Schmid, 2011; Fornara et al., 2010) and important morphological changes. For instance, the vegetative shoot apical meristem that produces leaves changes its identity and becomes an inflorescence meristem that produces reproductive organs for seed production. However, the important events for this developmental transition are not only confined to the shoot apical meristem (SAM). Indeed, physiological studies have shown that flowering time requires the whole plant system. Stimuli participating in the control of flowering time can be perceived by different organs in a complex signalling system (Bernier and Périlleux, 2005). The transition occurs once the SAM, which can be seen as a sink organ, integrates the signals and modifies its morphology.

The leaves are key organs in the control of floral transition. Indeed they are the organs involved in the light perception (intensity, quality, photoperiod) (Bernier and Périlleux, 2005; Li et al., 2016) and through their photosynthetic activity they are the major providers of various molecules. The leaf-produced compounds are gathered to the SAM and they trigger the floral transition trough a long-distance florigen signalling, via the phloem, to activate the key flowering-regulatory genes in the SAM (Song et al., 2015; Bernier and Périlleux, 2005; Li et al., 2016). The leaves could thus be described as source organs. In Arabidopsis, the photoperiod is one of the main factors inducing the developmental switch. In the leaf companion cells of the phloem, the light stimulus induces the expression of the *CONSTANS (CO)* transcription factor, which activates downstream regulators of the flowering time. *FLOWERING LOCUS C (FT)* is one of the CO targets, and is part of a long-distance signal (florigen) produced in the leaves, which converges to the SAM to activate genes involved in the floral transition switch. CO is also responsible for the mobilization of sugars during the floral transition (Ortiz-Marchena et al., 2014) and it has been demonstrated that increased levels of sucrose in leaves are triggered by inductive day-length (King et al., 2008; Corbesier et al., 1998).

However, sucrose is not the only metabolite involved in the floral transition, other carbohydrates also play an important role. Indeed, proteins involved in the carbohydrate synthesis are required during the inductive photoperiod in the leaves, in order to activate key flowering genes, such as *FT* and *TWIN SISTER OF FT* (*TSF)* (Wahl et al., 2013b). Cytokinins have also been shown to be present in leaves and their levels increase with the light stimulus and the induction of the floral transition (Bernier, 2013; Corbesier et al., 1998).

To decipher the complex flowering regulatory gene network, transcriptome analyses have been carried out mostly in meristem and root tissues in response to inductive light stimuli (Torti et al., 2012; Bouché et al., 2016; Schmid et al., 2003). There is a lack of data concerning similar flowering gene network in the leaf at the genome scale, despite the key role of this organ. To dissect the early transcriptional changes related to the floral transition in the leaves, we used a previously characterised short-day (SD) to long-day (LD) shift (Chapter 3) that induces a synchronized flowering. Genome-wide RNA-seq approach has been used to unravel the composition and the dynamics of the leaf gene network during the floral transition and to highlight the main molecular processes. We observed a large transcriptional reprogramming with major changes in photosynthetic activity, protein metabolism, DNA replication and chromatin organization. Interestingly, gene expression revealed a high endocycle-activity, in agreement with the changes in ploidy levels during the transition, which we previously recorded. Furthermore, a comparative analysis with transcriptome data acquired in shoot and root tissues during a similar floral transition was performed to enlarge the overview of the flowering gene networks and highlight specificities of the different organs in the integrated floral transition process. We highlighted common transcriptional changes in both organs pathways associated with the flowering time. This study provides an interesting and new source of candidate genes for further investigation of the early events of the floral transition.

Results

A SD-LD switch induces a large gene expression reprogramming in the second pair of leaves

To investigate the transcriptional events associated with floral transition in leaves we used a SD-LD shift that allows a controlled and synchronized induction of flowering (Corbesier et al., 1996). Before and after the transfer in LD we recorded the expression of key flowering genes to precisely define the floral transition window (Figure 1). The expression of *CONSTANS* (*CO*) and *FLOWERING LOCUS T* (*FT*), two key flowering time genes, peaked 3 days after the transfer and the expression of an early marker of the floral meristem, *APETALA 1* (*AP1)*, was detected after 5 days using an *AP1::GUS* transgenic line. The expression data and the characterisation of flowering time enabled us to define the floral transition window in this SD-LD switch between day 2 and day 5 (Figure 1). We thus chose the time points T0, T2, T3, and T5 to investigate the early events associated with flowering time in the second pair of leaves (see Chapter 3). We performed an RNA-seq experiment using Illumina paired-end and oriented sequencing. More than 40 millions of 100 bp reads were generated per sample. On average, 99% passed the quality filter and were uniquely mapped to the TAIR 10 reference genome (Supplemental table 1).

In the second pair of leaves, we identified 20 284 genes expressed in at least one of the four time points, corresponding to 60.4% of the 33 602 annotated genes in the *A. thaliana* nuclear, mitochondrial and chloroplastic genomes (Figure 2a). At each time point the number of expressed genes was quite similar. The vast majority of the expressed genes were protein coding (81.6%) and we noticed that 75.4% of the ncRNAs and 33.8% of the snoRNAs present in the genome were also expressed (Figure 2b).

We then identified 7 680 differentially expressed nuclear genes (DEGs) among the three comparisons T0/T2, T2/T3 and T3/T5, with the highest number at T0/T2, and no bias between upregulated and downregulated genes (Figure 3a). The comparison of the three gene sets allowed to identify a common set of 167 DEGs during the whole process, and three sets specific to the T0/T2, T2/T3 and T3/T5 transitions, with 5 326, 351 and 583 genes, respectively (Figure 3b).

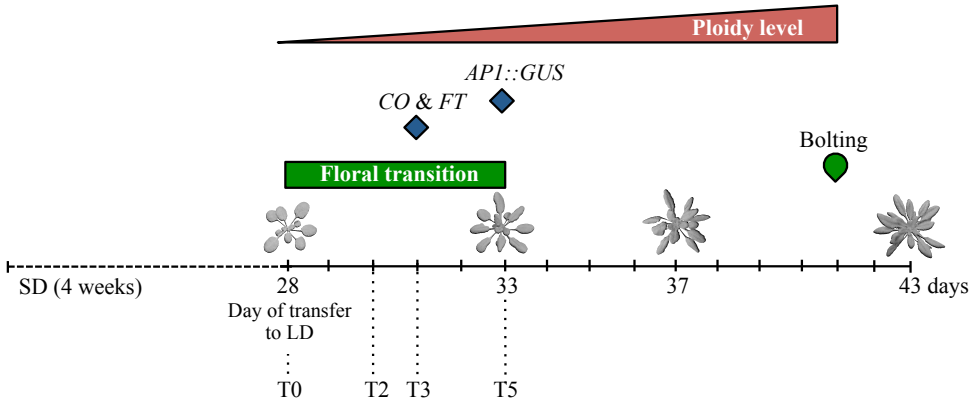

Figure 1: Chronology of the main events occurring during the SD-LD switch.
Plants were grown during 4 weeks in SD and then transferred in LD. The peak of *CO* and *FT* expression and the start of the expression of the floral meristem marker AP1 are indicated. Plants are bolting 13 days after the transfer in LD.

a)

Time point	Nr. of Nuclear genes	Nr. of Mitochondrial genes	Nr. of Chloroplastic genes	% total expressed genes	% of TAIR10 annotated genes
T0	19 831	36	73	97.8	59.0
T2	19 644	34	72	97.4	58.5
T3	19 707	37	76	97.7	58.6
T5	19 780	40	71	98.1	58.9

b)

	SD-LD switch			Genome (TAIR10)	
Sequence type	Nr. of expressed genes	% of total expressed genes	% of class genes	Nr. of genes	% of total genes
Protein coding	19 515	96.2	71.2	27 416	81.6
TE	206	1.0	5.3	3 903	11.6
Pseudogenes	200	1.0	21.6	924	2.7
tRNA	7	0.0	1.0	689	2.1
ncRNA	297	1.5	75.4	394	1.2
miRNA	28	0.1	15.8	177	0.5
snoRNA	24	0.1	33.8	71	0.2
rRNA	0	0.0	0.0	15	0.0
snRNA	7	0.0	53.8	13	0.0
Total	20 284			33 602	

Figure 2: Genes expressed in the second pair of leaves during the SD-LD switch.
a) Number and percentage of expressed nuclear, mitochondrial and chloroplastic genes at each time point.
b) Distribution of the types of sequences compared to the entire genome.

a)

Number of DEGs			
Comparison	**All**	**Up**	**Down**
T0/T2	6 582	3 322	3 260
T2/T3	1 012	470	542
T3/T5	1 673	703	970

b)

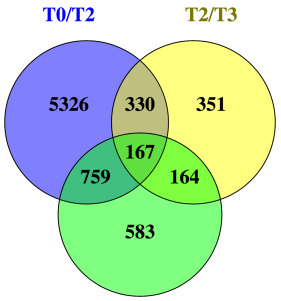

c)

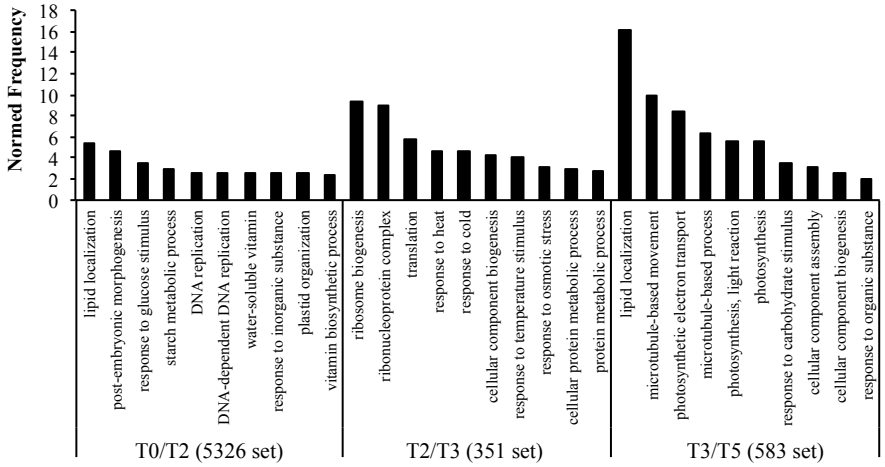

Figure 3: Genes differentially expressed during the floral transition in the second pair of leaves.

a) Differentially expressed genes (DEGs).

b) Venn diagram representing the overlapping and DEGs genes for each comparisons.

c) GO term enrichments analysis of the three specific DEGs sets using AgriGO tool. The top 10 biological process GO terms with the highest normed frequencies (NF) and p-value < 0.0001 are presented.

Number of DE-lncRNAs			
	T0/T2	**T2/T3**	**T3/T5**
No filter	307	5	20
DE (Bonferroni)	136	4	14
DE (BH)	329	5	29
Strand-	167	0	17
Strand+	162	5	12

Table 1: Number of differentially expressed lncRNAs (DE-lncRNAs).

The differentially expressed lnc transcript units have been detected without or with filter process using either Bonferroni or BH corrections.

These data highlighted that a large gene expression reprogramming was induced by the SD-LD shift and accompanied the floral transition in the second pair of leaves, with the largest change occurring at the T0/T2 transition.

Since long non-coding RNAs (lncRNAs) play important regulatory functions during development, we also searched for differentially expressed lncRNAs. Firstly, we established a large non-redundant dataset (IJPB_lncDS) of 14 621 lncRNAs (Supplemental figure 1a) and exploited the fact that the orientation of the transcripts was known in our RNA-seq experiment. We then remapped the reads on this dataset. In preliminary analyses, we could identify 348 DE-lncRNAs among T0/T2, T2/T3 and T3/T5. As expected for genes, the largest number of DE-lncRNAs was observed at T0/T2, without any bias in the strand orientation (Table 1). Further analyses are currently being performed to assess the genomic context of these DE-lncRNAs and the expression profiles of the neighbouring genes.

To better understand the evolution of the transcriptome profiles during the switch, we performed an analysis of the gene ontology (GO) terms of the 4 data sets, using the Classification SuperViewer from the Bio-Analytic Resource for Plant Biology (BAR) and the agriGO Analysis Toolkit (Figure 3c and Supplemental figure 2). The common set of 167 DEGs was enriched in the "response to stimulus and stress" (GO:0050896, GO:0006950, normed frequency (NF)=2.22 ± 0.245, p-value $2.6\ 10^{-8}$) with for instance genes involved in jasmonic acid (JA) biosynthesis and JA response, such as *JASMONATE-ZIM-DOMAIN PROTEIN* 1 (*JAZ1*) and 5 (*JAZ5*), *ALLENE OXIDE SYNTHASE* (*AOS*) and *ALLENE OXIDE CYCLASE 2* (*AOC2*), suggesting that the entire process is accompanied by a stress state. Interestingly, the 5 326 T0/T2 DEGs set did not present a major enrichment in specific GO terms using the BAR tool (Supplemental figure 2), but with agriGO the two highest terms detected were "lipid localisation" (GO:0010876, NF=5.32, p-value $5.8\ 10^{-7}$) and "post-embryonic morphogenesis" (GO:0009886, NF=4.66, p-value $9.3\ 10^{-8}$) (Figure 3c). In this data set we also found an enrichment of the GO term "DNA replication" (GO:0006260, NF=2.61, p-value $2.9\ 10^{-7}$), suggesting that a cellular reprogramming was occurring in the second pair of leaves during the developmental switch.

At T2/T3, enrichments in GO terms such as “ribosome biogenesis” (GO:0042254, NF=9.3, p-value $3.7\ 10^{-14}$) “ribonucleoprotein complexes” (GO:0022613 NF=8.9, p-value $8.9\ 10^{-14}$) and “translation” (GO:0006412, NF=5.8, p-value $9.3\ 10^{-37}$) suggested that the transition is accompanied by a strong modification of the protein metabolism. Among the 583 T3/T5 DEGs, a high enrichment of genes involved in “lipid localisation” (GO:0010876, NF=16.2, p-value $4.8\ 10^{-6}$) and “microtubule movement” (GO:0007018, NF=9.8, p-value $1.4\ 10^{-5}$) was observed, suggesting the presence of modifications at the cellular level. At T3/T5 genes involved in “photosynthesis” (GO:0015979, NF=5.6 p-value $5\ 10^{-7}$) were also detected, as well as at T0/T2 (GO:0009536, NF=1.7, p-value $1.4\ 10^{-43}$), thus a reprogramming of the photosynthetic machinery was induced by the SD-LD shift.

Nine gene clusters describe the transcriptional dynamics during the SD-LD switch

To further characterise the transcriptome profiles during the 5-day developmental window, we performed a hierarchical cluster analysis on the 7 680 DEGs based on their expression levels, using the MeV tool (Saeed et al., 2003). We identified 9 clusters (Figure 4), C6 and C5 being the largest ones with 3 171 and 2 369 DEGs, respectively, with contrasted opposite profiles. The majority of DEGs in C6 was repressed at T2 and the majority of DEGs in C5 activated at T2 and during the developmental transition. To better understand the functional specificities of the clusters, we performed a GO analysis. We found that a few clusters had strong enrichments in specific GO terms (Figure 5). For instance, C9 strongly differed from others with high enrichment in GO terms associated with “electron transport and energy pathway”, suggesting a strong rearrangement of the photosynthesis apparatus due to the SD-LD shift, already observed in the T3/T5 and T0/T2 specific GO terms. C2 cluster had the highest enrichment in “DNA and RNA metabolism” terms, such as “RNA processing” (GO:0006396, p-value $4.7\ 10^{-7}$), “RNA metabolism” (GO:0016070, p-value 0.0012) or “ribosome biogenesis” (GO:0042254, p-value 0.0032), thus the genes involved in the modification of gene regulation showed a rapid reversal of the expression profiles between T2 and T5.

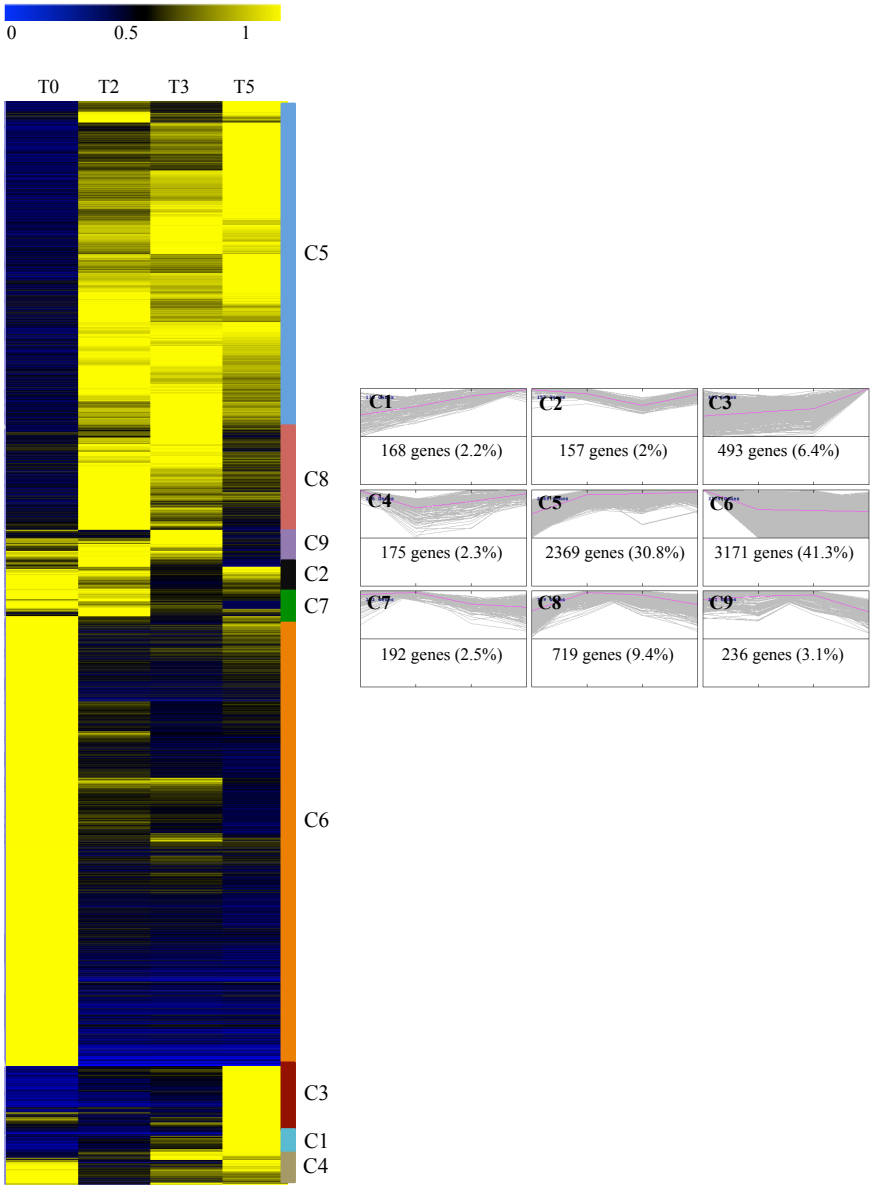

Figure 4: Clustering analysis of DEGs during the SD-LD developmental switch in the second pair of leaves.

a) Hierarchical clustering of the 7 680 DEGs based on their normalized mean expression values during the developmental transition.

b) Gene expression profiles in the nine clusters. The number of genes and the percentage of DEGs in each cluster were reported. Grey line, transcript profile of individual gene. Pink line, mean of the expression values of the genes present in the cluster.

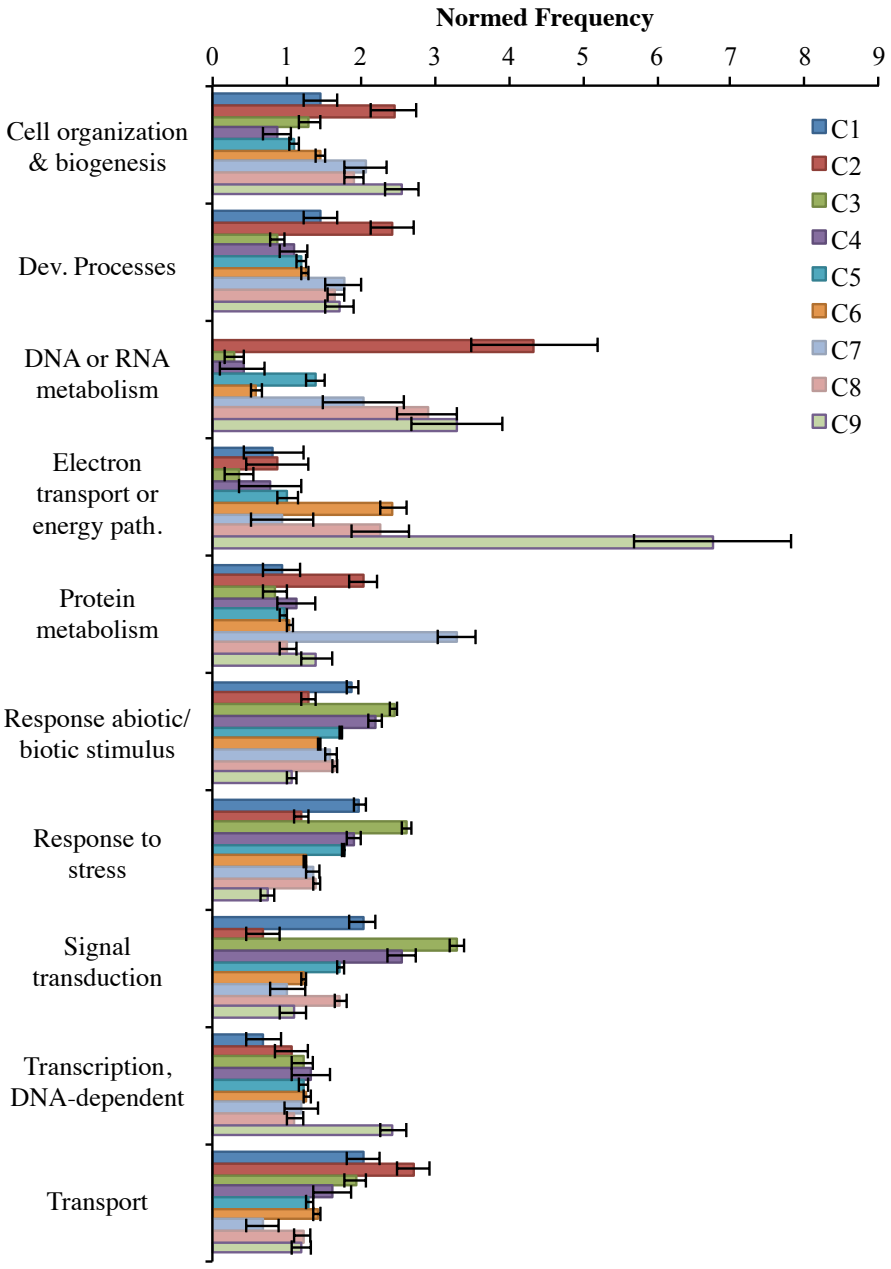

Figure 5: GO term enrichments in the nine clusters.
The BAR SuperViewer tool was used.

A “DNA replication” GO annotation (GO:0006260, p-value $2.8\ 10^{-11}$) was observed in C5. The C8 cluster characterised by transiently up- and down-regulated genes was enriched in GO terms associated to “chromatin organization” (GO:0006325, p-value $5.8\ 10^{-7}$) and “chromosome organization” (GO:0051276, p-value $4.2\ 10^{-7}$), suggesting a remodelling of the chromatin landscape during this short-time window. Genes downregulated two days after the LD shift were in the small C7 cluster, which was enriched in GO terms associated with protein metabolism such as “translation” (GO:0006412, p-value $9\ 10^{-37}$), “protein metabolic process” (GO:0019538, p-value $2.4\ 10^{-21}$) and “ribosome biogenesis” (GO:0042254, p-value $9\ 10^{-37}$). C1, C3 and C4 clusters, characterised by a continuous or transient upregulation of the genes, had similar enrichments in GO terms related to stress response and signal transduction. For instance, C3 was enriched in genes participating to the jasmonic (GO:0009753, p-value $2.8\ 10^{-11}$) and abscisic acid (GO:0009738, p-value $5.4\ 10^{-13}$) signalling pathways. Interestingly, “postembryonic development” GO annotation (GO:0009791) was significantly represented in C5 and C6. Among the postembryonic development genes the upregulated were related to flower development and flowering time whereas the downregulated were mostly involved in embryo development (GO:0009793, GO:0009553).

Specific transcription factor families involved in the developmental switch

Transcription factors (TFs) are important players to regulate gene expression during developmental transitions. We thus examined the distribution of TF families among the nine clusters. The list of TFs and the families they belong to were extracted from the Plant Transcription Factor Database (PlantTFDB http://planttfdb.cbi.pku.edu.cn), which contains 1 717 TFs classified into 58 families. Among the 7 680 DEGs of the three comparisons, we identified 518 TFs (i.e. 30% of the TFs database) belonging to 51 families. We thus highlighted some co-regulation of these different TFs during the developmental switch. The C1, C3, C4, and C5 clusters, which corresponded to continuous or transiently upregulated genes, contained the highest number of DE-TFs (Figure 6a).

a)

Cluster	Nr. gene	Nr. TFs	% TFs
C1	168	15	8.9
C2	157	3	1.9
C3	493	45	9.1
C4	175	18	10.3
C5	2 369	215	9.1
C6	3 171	170	5.4
C7	192	3	1.6
C8	719	36	5.0
C9	236	9	3.8

b)

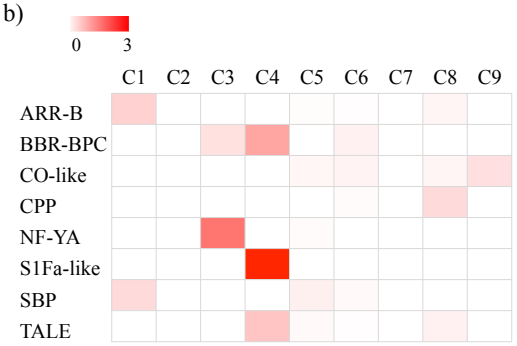

Figure 6: Distribution of transcription factors (TFs) in the nine clusters.
a) Number and percentage of TFs in each cluster.
b) Heat map of the TF families present in each cluster based on a normed frequency score taking into account the number of TFs in each class and the total number of TFs in the genome.

We observed that a few TF families were more represented in some clusters than in others (Figure 6b). For instance, C1 was characterised by the presence of RESPONSE REGULATOR 10 (AAR10) TF involved in the cytokinin signal transduction, which is important for the light response and shoot initiation (Argyros et al., 2008), SQUAMOSA PROMOTER BINDING PROTEIN-LIKE 3 (SPL3), which is a floral developmental regulator involved in the vegetative phase change, and four NAC TFs among which ARABIDOPSIS NAC DOMAIN CONTAINING PROTEIN 18 (ANAC018), which is involved in shoot development. The NF-YA TFs, involved in stress response in an abscisic-acid (ABA)-dependent manner, were present in cluster C3 with 6 members out of the 10 present in this family, confirming an alteration of the ABA metabolism during the SD-LD shift in the mature leaves. Indeed, it has been show that the ABA is an important flowering regulator in LD conditions (Riboni et al., 2014). BPC proteins were present among the differentially expressed TFs. Interestingly, *BASIC PENTACYSTEINE 6* (*BPC6*) and *BPC7,* involved in a wide range of biological processes, were upregulated during the floral transition in the leaves (present in clusters C3 and C4, respectively). The S1FA-like DNA-binding protein belonging to a novel class of TFs was present in C4, suggesting a possible new role of these TFs in floral transition. In C4 we found Homeodomain proteins belonging to the TALE TF family, such as KNOTTED1-LIKE HOMEOBOX GENE 4 (KNAT4) regulated by light and prominently expressed

in leaves, and surprisingly, BEL1-LIKE HOMEODOMAIN 9 (BELL1), which participates to the ovule identity. The clusters C5, C6, C8 and C9 were also enriched in CO-like TFs family that are involved in the integration of the photoperiodic signal and in the regulation of *CO*. CONSTANS-LIKE 9 (COL9*)* and COL5 are regulators of *CO* and *FT* expression and were present in C5 and C6, respectively. Another CO-like TF important for the light perception, *COL1* was upregulated during the transition. The cysteine-rich polycomb-like (CPP) TF family was present in the C8 cluster, with TSO1-like proteins SOL1 (AT3G22760) and TCX2 (AT4G14770). TSO1 is involved in the control of cell growth and division and in the development of reproductive organs (Hauser et al., 2000; Lu et al., 2013), therefore, SOL1 and TCX2 may be interesting candidates to participate to the floral transition. Among the differentially expressed TFs, even if less represented, we also observed TFs from the GRAS or BES1 families that mediate brassinosteroid gene regulation, as well as TFs of TCP and E2F families, important for cell proliferation. The TFs of these families were mostly upregulated in C5. Surprisingly, only a small percentage of MADS TFs was found among DEGs.

Expression of flowering genes in leaves in response to the SD-LD switch

To better characterise our leaf transcriptome, we established a 352-gene dataset, hereafter dubbed FIORE, related to flowering time based on FLOR-ID (Bouché et al., 2015), ThaleMine resource (ARAPORT) and bibliography (Figure 7a). The FIORE flowering genes (FLGs) are involved in different regulatory pathways and were organised in classes according to the pathway they belong to, as described in FLOR-ID and bibliography. In our dataset a small percentage (5% of the FIORE dataset) corresponded to genes involved in flower meristem identity and flower development. Among the 20 284 loci expressed in the second pair of leaves, we identified 307 FLGs expressed during the developmental switch (87% of the FIORE dataset) and a total of 127 differentially expressed genes (DE-FLGs) in the three main T0/T2, T2/T3 and T3/T5 comparisons, with no bias between up- and down-regulated genes (Figure 7b). The largest transcriptional reprogramming occurred between T0/T2, with 111 DE-FLGs involved in all regulatory pathways.

a)

Database	Nr. AGI	References
FLOR-ID	306	Bouché et al.. 2015
ThaleMine	82	www.araport.org
Complement dataset	18	Based on bibliography
FIORE	352	Non redundant AGIs from the 3 datasets. This work.

b)

Number of DE-FLGs			
Comparison	**All**	**Up**	**Down**
T0/T2	111	59	52
T2/T3	19	12	7
T3/T5	16	7	9

c)

Pathways name	Nr. Genes in FIORE	DE-FLGs in leaves	% DEGs T0/T2	% DEGs T2/T3	% DEGs T3/T5
Photoperiod	119	52	39.5	5.9	3.4
General & Autonomous	127	28	21.3	1.6	0.8
Hormones	33	18	45.5	9.1	15.2
Circadian Clock	23	15	56.5	21.7	4.3
Aging	22	7	31.8	0.0	0.0
Flower Dev. & Meristem Id.	18	6	11.1	5.6	16.7
Flowering Time Integrators	8	6	50.0	25.0	25.0
Vernalization	27	3	11.1	3.7	0.0
Sugar	9	3	33.3	0.0	11.1
Ambient Temperature	7	3	42.9	0.0	0.0

d)

Cluster	Nr. FLGs	% in the cluster	Gene symbols
C1	7	6	*AT4G36590, BFT, FT, MYR2, SPL3, TSF*
C2	1	1	*CCA1*
C3	3	2	*AGL8, CPK6, GID1B*
C4	4	3	*ELF4, FUS9, GID1A, MAF5*
C5	47	37	*AGL24, AP2, CO, LHY, RVE2, SPA3, SPA4, TEM1,*
C6	49	39	*AGL20, GI, PRR5, PRR7, SMZ, SPL4, SPL9, SVP, TOE, GID1C*
C7	2	2	*AGL87, AT1G69570*
C8	11	9	*AT1G75060 , ATH1, COL2, GAMT2, MYB30, RBP-DR1, ULT1, VIM1, VIM3*
C9	3	2	*AT5G14920, FBH4, GASA6*

Figure 7: Flowering genes and their expression during SD-LD switch.
a) Composition of the FIORE data set and associated references of the databases used to establish FIORE.
b) Number of differentially expressed genes related to flowering (DE-FLGs).
c) Distribution of the flowering genes in pathway classes.
d) Distributions of the DE-FLGs in the nine clusters. A selection of FLGs is given for each cluster.

A large subset was involved in the photoperiodic pathway (39.5% of the class) and one of the most represented pathways was the circadian clock class with 56.5% genes of the class (Figure 7c). Minor changes were observed in terms of gene number in the T2/T3 and T3/T5 comparisons (Figure 7b). Interestingly, the representation of the "flower-development and meristem identity" class increased during the developmental window, which was expected in meristem but not in the leaf tissues. The aging and ambient-temperature classes were only associated with the T0/T2 transition, possibly due to the environmental change and the transient stress response (Figure 7c).

We then investigated more precisely the expression profiles of the 127 DE-FLGs (Figure 7d). In cluster C1, *FT* was co-regulated with 5 other TFs, such as BRO*THER OF FT* (*BFT*), *TWIN SISTER OF FT* (TSF), *SPL3* but also some new TFs such as the homeobox MYR2 TF or the MADS-box AT4G36590 TF. *CO* was co-regulated with 46 other genes in cluster C5. Sixteen genes were downregulated with different kinetics during the process, belonging to clusters C7, C8 and C9, such as the epigenetic regulators of the flowering time *VIM1* and *VIM3*. Among this small set of genes we found AT1G75060, which encodes an unknown protein and, based on Panther Classification prediction, belongs to the histone deacetylase complex subunit SAP30L subfamily. These data provide new regulatory candidates in leaf involved in floral transition signalling beside the well-described *CO* and *FT* regulators. Among the "flowering integrator" class, the positive flowering regulators *FT*, *TSF*, *AGL24* were activated whereas *AGL20/SOC1*, another positive regulator, was surprisingly downregulated and showed a similar profile to the negative regulator *SVP*. *MAF5,* a negative regulator of the vernalization pathway, was transiently downregulated in the first two days after the transfer and then upregulated from T2 to T5. Among the clock components the *CCA1, LHY* and *RVE2* negative flowering regulators were upregulated whereas the *GI*, *PRR5* and *PRR7* positive flowering regulators were downregulated. Half of the members of the photoperiod pathway (25) were present in cluster C5: they were activated by the light shift and expressed during the entire developmental process.

During the switch, the genes involved in gibberellin (GA) biosynthesis were mainly downregulated, while enzymes involved in the GA catabolism or GA modifications were activated, suggesting a change in GA level and composition,

whereas negative regulators of GA responses were upregulated (Supplemental table 2). Two gibberellin receptors were detected, which were upregulated with different kinetics, *GID1A* and *GID1B*, belonging to clusters C4 and C3, respectively, suggesting that they may be required during the transition and that they have some specialized functions regarding the developmental switch. In parallel, we observed the activation of genes involved in cytokinin (CK) biosynthesis and of the *SOB FIVE-LIKE 1, 2* genes, which led to the increase of CK levels (Zhang et al., 2009). Genes involved in CK catabolism (*CKK4*, *CKK6*) were downregulated consistently with the role of CK in flowering (Supplemental table 2). Interestingly, whereas gibberellins were proposed to promote floral transition, our data suggest that during the floral transition induced by the SD-LD switch, the balance between GAs and CKs and the composition in the different forms, rather than their absolute levels, was likely to be critical.

We then compared our data with differentially expressed genes identified in meristem (Torti et al., 2012) and roots (Bouché et al., 2016) during a similar developmental window, where a photoperiodic switch induced the flowering time. Torti et al. (2012) established a list of 202 genes upregulated after the LD shift in micro-dissected meristems committed to floral transition. A comparison with the DEGs identified in leaves allowed to extract 28 genes upregulated both in committed meristems and in leaves at the T0/T2 transition (Table 2), suggesting some common mechanism in the two tissues resulting from the SD-LD shift. One third of these genes were unknown, thus their upregulation in both tissue during the transition suggests that they have a function in this switch. Among them, 5 were encoding TFs such as: WOX3/PRESSED FLOWER (PRS), a plant-specific WUSCHEL-related homeobox involved in flower and leaf development (Costanzo et al., 2014); POPEY, a TF involved in iron-deficiency response (Long et al., 2010); and RGA-LIKE1 (RGL1), a DELLA protein interacting with WRKY12 and WRK13, two TFs involved in the control of flowering under SD conditions (Li et al., 2016).

Locus Up regualted in meristem and in T0/T2 transition	Function
GAMMA RESPONSE GENE 1 (ATGR1)	Cell cycle, endoreduplication, DNA damage
INFLORESCENCE MERISTEM RECEPTOR-LIKE KINASE 2 (IMK2)	Leucine-repeat receptor kinase
NITRATE REDUCTASE 2 (NIA2)	Nitrate metabolism
AMINOPHOSPHOLIPID ATPASE 1 (ALA1)	Putative aminophospholipid translocase
WUSCHEL RELATED HOMEOBOX 13 (WOX13)	TF
WRKY16	TF
POPEYE (PYE)	TF (bHLH)
RGA-LIKE 1 (RGL1)	TF (GRAS)
AT4G32670	TF (RING/FYVE/PHD zinc finger)
AT4G22770	TF (AT hook motif)
AT1G11380	PLAC8 family
AT1G34110	Leucine-rich receptor-like protein kinase family protein
AT1G58848	Disease resistance protein (CC-NBS-LRR class) family
AT1G66180	Putative aspartyl protease
AT1G71180	6-phosphogluconate dehydrogenase family
AT3G10840	Alpha/beta-Hydrolases superfamily
AT3G25600	Calcium-binding EF-hand family
AT5G25170	PPPDE putative thiol peptidase family protein;
AT1G70480	Unknown
AT2G40820	Unknown
AT2G47820	Unknown
AT4G15545	Unknown
AT4G22130	Unknown
AT5G05240	Unknown
AT5G10150	Unknown
AT5G56120	Unknown
AT5G65990	Unknown
AT4G33560	Wound-responsive family protein

Table 2: List of genes upregulated both in meristem and leaves during the SD-LD developmental switch.
The upregulated genes in dissected meristem were extracted from Torti et al. (2012).

In the work of Bouché et al. (2016), 595 genes were differentially expressed in roots 22 hours after the SD-LD floral inductive shift. We searched for common pathways in both tissues involved in the early events of the floral transition and identified 350 genes present in Bouché's dataset and in the T0/T2 comparison with similar or opposite expression profiles (Figure 8). For instance, 92 genes were downregulated in roots and upregulated in leaves and mostly involved in metabolic processes and in the regulation of transcription. Five out of 14 TFs detected in this subset of genes were MYB-related genes, such as *LCL1* and *RVE1* regulators of the circadian rhythm and synergistically working with CCA1 and LHY. Among the 350 genes, 52 genes were upregulated in both tissues (Figure 8), highlighting some coordinated regulation in the two tissues in response to the shift. Interestingly, three TFs were identified: HY5, participating to the photoperiod response and with a putative role on ABA responses;

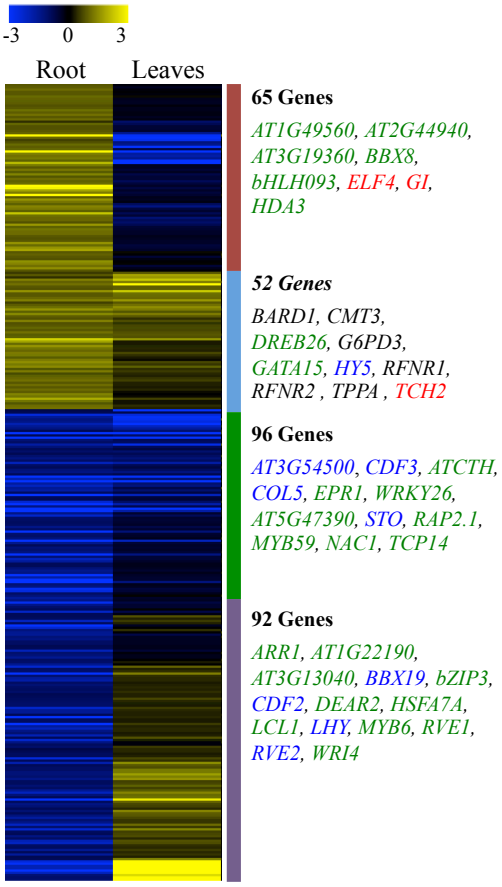

Figure 8: Heat map of the DEGs in root and leaves during the SD-LD developmental switch.
Log2 (Fold-Change) of the T0/T2 transition for leaf and root (Bouché et al., 2016) have been used. The number of genes with a specific expression profile in both tissues is indicated. Transcription factors (in green), FLGs (in red), TFs and FLGs (in blue) are reported for the four main gene clusters.

DEHYDRATION RESPONSE ELEMENT-BINDING PROTEIN 26 (DREB26), belonging to the ERF/AP2 transcription factor family involved in the response to external stimuli; and GATA15, involved in cytokinin signalling (Ranftl et al., 2016).

These 52 upregulated genes in both root and leaf tissues were enriched in genes participating to catalytic activity. Among them we can cite: G6PD3, a glucose phosphatase; RFNR1 and RFNR2, root specific ferredoxin NADP(H)

a)

DE-Chromatin-associated genes			
Comparison	**All**	**Down**	**Up**
T0/T2	82	19	63
T2/T3	6	4	2
T3/T5	22	18	4

b)

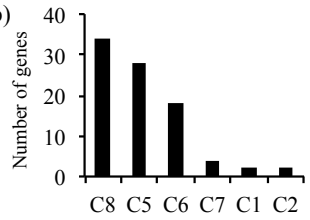

c)

	Dataset	DEGs at T0/T2			DEGs at T2/T3			DEGs at T3/T5		
Class	**Total number**	**All**	**Down**	**Up**	**All**	**Down**	**Up**	**All**	**Down**	**Up**
Histone code	70	11	3	8	4	3	1	1	0	1
Histone	55	33 (60.0%)	4	29 (52.7%)	0	0	0	15 (27.3%)	14	1
CR machine	49	6	1	5	2	1	1	0	0	0
Transcription	44	8	3	5	0	0	0	1	0	1
Structure	37	13 (35.1%)	6	7	0	0	0	4	3	1
Silencing	26	8 (30.8%)	2	6	0	0	0	1	1	0
DNA modif	15	3	0	3	0	0	0	0	0	0
Others	13	0	0	0	0	0	0	0	0	0
Total	309	82	19	63	6	4	2	22	18	4

Figure 9: Chromatin-associated genes and their expression during the SD-LD switch.
a) Number of differentially expressed genes related to chromatin (CA).
c) Number of CA-DEGs in the nine clusters.
d) Distribution of CA-DEGs in the different chromatin classes

oxidoreductases, whose expression is induced by nitrogen and carbon metabolites (Girin et al., 2007); and TPPA, involved in trehalose biosynthesis and regulated by light stimuli and sucrose levels (Van Houtte et al., 2013).

Chromatin-associated genes deregulated during the SD-LD switch

Since chromatin plays a critical role in the control of gene expression during developmental phase transitions, in our dataset we analysed the expression profiles of genes associated with chromatin. Among the 309 chromatin-associated genes (CAGs) organised in 8 classes according to their functions (Chupeau et al., 2013), 90 were differentially expressed and most of them (91%) were present in T0/T2, suggesting a rapid modification of the epigenome concomitant with the transcriptional reprogramming. Minor changes were observed in T2/T3 (6 genes) and T3/T5 (22 genes). The balance between up- and down-regulated genes was not conserved in T0/T2 and T3/T5, suggesting

specific expression patterns among the differentially expressed chromatin-associated genes (DE-CAGs) (Figure 9a). For instance, most of the DE-CAGs (34) were in cluster C8, suggesting that a transient change of their expression profiles accompanies the environmental changes and the floral transition (Figure 9b). The DE-CAGs in C6 (18) and C7 (4) were mostly downregulated, meaning that their functions were not required during the process. However, we detected 28 CAGs in the C5 cluster, which were upregulated and thus putatively involved in the developmental switch.

All classes of chromatin-associated genes were present in T0/T2 DEGs (Figure 9c) with some classes more represented such as histones (60%), chromatin structure grouping proteins involved in nucleosome/chromatin assembly (35.1%) and the silencing class (30.8%), with genes participating to the transcriptional silencing. Genes encoding histones were also well represented in T3/T5 DEGs (27.3%), but most of the histone genes were upregulated at T0/T2 and downregulated at T3/T5 (Figure 9c). Only few histone variants were downregulated at T0/T2 and interestingly, the histone H3-1 variants were mostly upregulated during this early phase (Table 3). These data suggest a drastic change in histone composition during the floral transition.

The class of DEGs involved in histone modifications was enriched in histone deacethylase (HDAC) encoding genes. Five HDACs (out of the 16 present in the dataset) were deregulated, namely *HDA2*, *HDA5*, *HDA8*, *HDT1* and *HDT4* (Supplemental table 4). *HDA5* was upregulated at T0/T2 (belonging to the C5) and *HDA8* was continuously upregulated over time (belonging to the cluster C1 as *FT*). The HDT1 (also named HD2A or HDA3) histone deacetylase involved in development (leaf polarity, embryo, seedling) showed an opposite expression profiles between T2 and T5. The two histone acetyltransferases *HAC5* and *HAG2* had antithetical expression profiles. It has been shown that modifications in DNA methylation to accompany the early events of floral transition. Consistently, we detected an upregulation of *MET1*, *CMT3* but also of *DEMETER-LIKE2* (*DML2*), encoding a DNA glycosylase involved in active DNA demethylation. Interestingly, *CMT3* was activated both in leaf and root tissues (Supplemental table 3). Some of the genes encoding Polycomb and Trithorax proteins were also deregulated such as *EMF1*, *SDG4* or *ULT1*.

Gene ID	Symbol	Family	T0/T2 log2Fold Change	T2/T3 log2Fold Change	T3/T5 log2Fold Change
AT2G18050	HON3	histone H1-3	1.01		0.78
AT5G59870	HTA6	histone H2A	1.12		-0.49
AT2G38810	HTA8	histone H2A	1.03		-0.31
AT3G54560	HTA11	histone H2A	0.91		-0.23
AT1G51060	HTA10	histone H2A	0.64		-0.44
AT3G20670	HTA13	histone H2A	0.61		-0.34
AT5G27670	HTA7	histone H2A	0.58		-0.41
AT4G27230	HTA2	histone H2A	0.53		-0.31
AT5G54640	HTA1	Histone H2A (RAT5)	0.52		-0.37
AT1G08880	HTA5	Histone H2A-X	0.32		-0.11
AT5G22880	HTB2	histone H2B	1.37		-0.19
AT5G02570	HTB10	histone H2B	1.01		-0.38
AT3G53650	HTB6	histone H2B	0.93		-0.50
AT3G46030	HTB11	histone H2B	0.43		-0.29
AT3G45980	HTB9	histone H2B	0.34		-0.34
AT5G59910	HTB4	histone H2B	0.33		-0.17
AT1G01370	HTR12	Histone H3 (CENH3)	0.67		-0.30
AT5G65360	HTR1	Histone H3 (H3.1)	1.07		-0.30
AT5G10400	HTR13	Histone H3 (H3.1)	1.03		-0.46
AT1G09200	HTR2	Histone H3 (H3.1)	0.98		-0.39
AT5G10390	HTR9	Histone H3 (H3.1)	0.96		-0.05
AT3G27360	HTR3	Histone H3 (H3.1)	0.92		-0.57
AT5G59690	HFO2	histone H4	1.03		-0.30
AT3G46320	HFO1	histone H4	0.85		-0.46
AT3G45930	HFO7	histone H4	0.85		-0.31
AT5G59970	HFO6	histone H4	0.78		-0.43
AT2G28740	HFO3	histone H4	0.72		-0.54
AT1G07820	HFO4	histone H4	0.45		-0.35
AT3G53730	HFO5	histone H4	0.35		-0.32
AT5G02560	HTA12	histone H2A	-0.39		0.10
AT2G30620	HON2	histone H1	-0.39		-0.13
AT5G08780	HON8	histone H1	-0.52		0.01
AT2G28720	HTB3	histone H2B	-1.75		-0.05
AT1G07790	HTB1	histone H2B			-0.40
AT2G37470	HTB5	histone H2B			-0.47

Table 3: List of histone-related genes deregulated during the developmental switch. Log2 (Fold-Change) are reported. Black cells indicate non-statistically significant fold change values. Yellow and blue cells indicate statistically significant positive and negative fold change values, respectively.

Gene ID	Symbol	Name	T0/T2 log2Fold Change	T2/T3 log2Fold Change	T3/T5 log2Fold Change	Cluster
GO:0042023 - DNA endoreduplication						
AT1G47870	E2Fc		0.58			C5
AT3G19150	KRP6	KIP-related protein 6	0.71			C5
AT3G48160	DEL1	DP-E2F-like 1	0.83			C5
AT3G50630	KRP2	KIP-related protein 2	0.53			C5
AT1G15570	CYCA2;3	CYCLIN A2;3	-0.79		-0.94	C6
AT2G27960	CKS1	cyclin-dependent kinase 1	-0.51	0.32		C6
AT2G42260	UVI4	UV-B-INSENSITIVE 4	1.16			C8
GO:0032876 - negative regulation of endocycle						
AT3G15150	HPY2	HIGH PLOIDY2	0.68			C5
AT2G18290	APC10	anaphase promoting complex 10	-0.94			C6
AT1G33240	GTL1	GT-2-like 1	0.50		-0.37	C8
GO:0032877 - positive regulation of endocycle						
AT3G10525	LGO	LOSS OF GIANT CELLS FROM ORGANS	1.17	0.29		C5
AT3G24810	ICK3	Cyclin-dependent kinase inhibitor 3	0.87			C5
AT4G02980	ABP1	ER auxin binding protein 1	0.34			C5
AT1G55350	DEK1	DEFECTIVE KERNEL 1	0.33			C8
GO:0032875 - regulation of endoreduplication						
AT1G78770	APC6	anaphase promoting complex 6	0.65			C5
AT1G19270	DA1	DA1	-0.95			C6
AT1G69380	RRG	RETARDED ROOT GROWTH	-0.39			C6
AT5G11510	MYB3R-4	myb domain protein 3r-4	0.47		-0.68	C9

Table 4: List of differentially expressed DNA endoreduplication-related genes.
Log2 (Fold-Change) is reported. Black cells indicate non-statistically significant fold change values. Yellow and blue cells indicate statistically significant positive and negative fold change values, respectively.

Endoreduplication is enhanced during the inductive SD-LD switch in leaves

We previously characterised the leaf growth during the inductive SD-LD shift and observed a significant increase of the endoreduplication factor in the second pair of leaves (see Chapter 3). We thus examined the profiles of genes related to endoreduplication using annotations from the ThaleMine database. Eighteen genes were deregulated among the 37 DNA endoreduplication-related genes present in the database and associated to the following GO terms GO:0042023, GO:0032876, GO:0032877, GO:0032875. The positive-endocycle regulators were mainly upregulated, such as *ER AUXIN BINDING PROTEIN1*

(*ABP1*), *LOSS OF GIANT CELLS FROM ORGANS* (*LGO*) and *E2Fc*, a mitotic inhibitor. Consistent with the deregulation of genes associated with endoreduplication, the deregulation of the major cell-cycle markers suggested an alteration of the mitotic cell-cycle. The *E2Fb* TF, involved in the activation of S phase was upregulated, along with *TIL1* another positive regulator of the S phase and *TSO2*, known to be predominantly transcribed during the S-phase and involved in the dNDP biosynthesis during DNA replication. Genes involved in the progression of the G2/M phase, such as *NRP2*, *CDKB2.1*, *CYCA1;1* were downregulated, while *WEE1,* a negative regulator of the entrance in the M phase, was upregulated, suggesting the arrest of cytokinesis. Interestingly, the *KRP2* and *KRP6* cell cycle inhibitor genes, shown to be involved in the progression of the endocycles through inhibition of CDKA (Verkest et al., 2005), were also upregulated. Finally, it was previously shown that the onset of endocycles requires the down regulation of *CYCA2;3* and *CYCD3.1* (Dewitte et al., 2003; Imai et al., 2006). Consistently with these data and the observation of endoreduplication in leaves, the two cyclin genes were indeed downregulated at T0/T2. Thus, our transcriptome data suggested an active DNA replication with predominant endocycles, consistent with our cell sorter analysis.

Discussion

Complexity of the floral transition process at the leaf level

The SD-LD exposure switch allows to study the early events triggering floral transition. The combination of this inductive system with the use of the high-throughput RNA-seq approach supplied for the lack of transcriptional data in mature leaves during this developmental switch. A large set of differentially expressed genes were detected and grouped in nine clusters with peculiar expression patterns and characterised by specific GO-terms enrichment. The floral transition induced by the SD-LD switch is accompanied by a transcriptional reprogramming of genes that are involved in photosynthesis, lipid localisation, protein metabolism and stress response, highlighting the complexity of this developmental switch. Photosynthetic components were shown to be required for flowering responses (Ortiz-Marchena et al., 2015; Wahl et al.,

2013a; Bernier and Périlleux, 2005). Furthermore, Corbesier et al. (1998) showed that the leaf carbohydrate level increases rapidly but transiently after the LD exposure. Some photosynthates affect the expression of key flowering genes such as *FT* (Wahl et al., 2013a), thus they are probably produced in an early phase of the transition. In agreement with these data, the genes involved in the photosynthetic processes and in the response to glucose stimulus in leaves were activated just after the SD-LD switch. Fatty acids and lipids are important molecular players involved in growth and development. In this work, we surprisingly identified DEGs associated with lipid-location GO-terms, suggesting a putative role of these genes in the floral transition. Interestingly, FT belongs to the phosphatidyl ethanolamine-binding protein (PEBP) family. It would be interesting to investigate whether other proteins encoded by genes belonging to the "lipid localisation" GO term participate to a florigen signalling in leaf. Reverse genetic approaches could bring preliminary data to select the best candidates based on their flowering-time phenotypes.

We reported a complex array of 518 TFs forming a transcriptional network possibly associated with floral transition. A large diversity of TFs involved in the regulation of various processes was identified, consistently with the molecular processes highlighted with the GO analysis. Numerous TFs involved in the regulation of homeotic genes were detected such as BPC6, which works in concert with LIKE HETEROCHROMATIN PROTEIN1 (LHP1), a PRC1 subunit, to regulate homeotic genes involved in the reproductive development (i.e. *AG, SEP3*) (Hecker et al., 2015). The *BPC6* upregulation detected in the leaves could suggest its participation in the regulation of the early phase of this developmental transition. TFs and genes involved in the phytohormone ABA signalling were, as well, upregulated during the switch, suggesting an alteration of the ABA pathway. ABA signalling proteins involved in the control of flowering time have been previously described and it was shown that ABA is an important factor influencing flowering time in LD conditions, by regulating key flowering genes, such as *FT*, *CO* and *GIGANTEA* (*GI*) (Riboni et al., 2014, 2013). Moreover, we also observed the upregulation of the flowering gene *HY5*, both in leaves and in root (Bouché et al., 2016), whose transcript level is modulated by an ABA treatment (Carrio-Seguı et al., 2016). The atlas of TFs identified as deregulated during the floral transition in the leaves, as well as, the

unknown proteins identified in both meristem and leaf, provide new candidates with putative roles in the SD-LD switch.

This transcriptional reprograming is likely accompanied by chromatin reorganization as suggested by deregulated genes involved in chromatin composition and remodelling, histone code or DNA methylation. Chromatin rearrangements at the nuclear level were observed during the floral transition in leaves and reported by Tessadori et al. (2007). Here, we highlight the actors of these chromatin rearrangements.

Specific expression patterns of flowering genes in leaves

Resetting of the phase of the clock with the SD-LD switch seems to have a large impact on circadian clock genes. Indeed, 65.2% of the circadian-associated genes of FIORE were deregulated, with major upregulation of *REV8* and the MYB-like TF *LHY* (log2 fold changes of 4.5 and 3.9, respectively) and downregulation of *GI*, *PRR3, 5, 7*, and *PRR9*, consistently with the repressive role of PRR5, PRR7 and PRR9 on *LHY* expression. Furthermore circadian clock genes are also regulated by the accumulation of photosynthates and different metabolites (Haydon et al., 2013). Whether this deregulation is due to a change in photosynthesis activity or in the clock itself remains to be established. Interestingly, other studies also showed that after the photoperiodic switch there is an alteration on the rhythmicity of gene expression (Bouché et al., 2016). It is known that LHY can stimulate flowering under LD conditions by activating *FT* expression (Fujiwara et al., 2008), while, the role of the clock-gene activator TF REVEILLE 8 in floral transition and florigen signalling is interesting to challenge.

Besides *FT* and *CO*, the key flowering genes *TSF* and *AGL24* were among the most upregulated genes at T0/T2, suggesting a strong co-regulation during the switch. The expression patterns of *CO*, *FT* and *SVP* (Supplemental figure 4) were in agreement with literature as well as our previous results (see Chapter 3). *SOC1* expression was firstly repressed at T0/T2 and then slightly activated. Recently, it has been demonstrated that *SOC1,* is also expressed in protoplasts of stomata guard cells with a role in the enhancement of stomata aperture (Kimura

et al., 2015). Since the photosynthetic activity enhances the stomata aperture, the slight *SOC1* activation may be due to this process. Besides these well-known integrators, other FLGs could be classified according to their expression patterns, thus highlighting the timing of their roles during the switch.

From our transcriptional comparative analysis between leaves, root and meristem tissues during similar floral transition window, we highlighted some common deregulated genes with a role on the early phase of the floral transition. Genes involved in catalytic activity were detected, such as *PYE,* that helps to maintain the iron homeostasis and is involved in the response to iron-deficiency (Long et al., 2010). The homeostasis of iron is strictly regulated since it can impact plant growth and development, as well as the length period of circadian rhythm (Chen et al., 2013). For instance, clock components such as *CCA1*, *LHY*, and *GI* modulate their expression in response to iron availability (Chen et al., 2013). Therefore, the deregulation of the clock genes, which is concomitant with *PYE* upregulation, both in leaves and meristem, could suggest a new role for PYE in flowering time.

Changes in endocycles activity

The histone transcript levels in the leaves increased during the first two days in LD. Similar changes were observed in 11-day-after-germination apical meristems (M5 stage), which showed a peak of cell-division activity and histone-gene expression during the floral transition window (Klepikova et al., 2015). Interestingly, several genes encoding H3.1 histone variants, which are incorporated during DNA replication, were upregulated, suggesting an active replication activity in the leaves during the T0/T2 transition. During our floral window the global upregulation of histone genes occurred concomitantly with the upregulation of other S phase markers, suggesting a burst of DNA replication in the early phase of floral transition. The overexpression of genes involved in DNA replication can lead the cell progression towards the mitotic cell-cycle or endocycle (Castellano et al., 2004; Schnittger et al., 2002), the two processes sharing common DNA replication machinery. In our data set we also observed the upregulation of specific markers associated with endocycle, suggesting a redirection of leaf cells towards endoreduplication, in agreement with the

increased ploidy level observed during the switch in the leaves (see Chapter 3) and with the increase in nuclear volume (data not shown). Therefore, despite some common traits between meristem and leaf, during the floral-transition window the two organs differ in their strategy after DNA replication. It remains to be established how and to which extent endoreduplication, which participates to cell size, differentiation and more metabolically active cells (Lee et al., 2009; Orr-weaver, 2016), contributes to floral transition.

Future perspectives

Our data highlighted gene networks that control the molecular events accompanying the floral transition on mature leaves and provided a set of new candidate genes. Further characterisation at the molecular level and by reverse-genetic approaches will clarify the role of these candidates on flowering. Using our RNA-seq data, we initiated an analysis of the differentially expressed lncRNAs, and identified new lncRNA candidates whose regulatory role in flowering time will be investigated. Finally, our leaf-specific transcriptome data provides a new resource for large-scale computational data-mining analysis to further understand the sophisticated relationships of the gene regulatory network during development and in response to external cues.

Experimental procedure

Plant material and growth conditions

Plants of *A. thaliana* ecotype Col-0 were grown in soil, in growth chamber with white fluorescent light, under short-day (8 hours light/16 hours dark, SD) for 4 weeks and then transferred in long-day (16 hours light/8 hours dark, LD). Temperature in SD was 21°C during the light period and 18°C during the dark, humidity (65%) remained constant. In LD, temperature (21°C) and humidity (70%) remained constant. Plants were analysed at different time points before and after the transfer, and leaf material was collected before dusk, at Zeitgeber time 15 (ZT15), considering ZT 0 as the ON switch of the light.

RNA extraction, library preparation and sequencing

Total RNA from the 3rd and 4th was extracted with the Plant RNeasy Mini kit (QIAGEN). 10 µg of RNA was treated with TURBO DNA-free kit (Ambion Ref. AM1907) and cleaned-up from enzymatic reactions with RNeasy MinElute Cleanup Kit (QIAGEN Ref. 74204), following the manufacture instructions. RNA integrity and concentration was analysed with the Agilent 2100 Bioanalyzer using the Agilent RNA 6000 Nano Kit (Ref. 5067-1511). To produce one replicate, the second pairs of leaves were dissected from 20 plants and pooled. Three independent replicates were performed for each time point.

100-bp oriented paired-end sequencing was performed on an Illumina HiSeq2000 machine. The oriented libraries were prepared from polyA RNAs using the Illumina Tru-Seq RNA sample preparation v2 kit and multiplexed. Four libraries were sequenced per lane.

RNA-seq data analysis

Each RNA-seq sample followed the same pipeline from trimming to count of transcript abundance as follows. The read preprocessing criteria included trimming library adapters and performing quality control checks using FastQC. The raw data (fastq) were trimmed by fastx toolkit for Phred Quality Score > 20,

read length > 30 bases. The mapper Bowtie version 2 (Langmead and Salzberg, 2012) was used to align reads against the *A. thaliana* transcriptome. We extracted 33 602 genes from TAIR10 version database (Lamesch et al., 2012), with one isoform per gene corresponding to the representative gene model (longest CDS) given by TAIR10. The abundance of each gene was calculated by a local script which parses SAM files and counts only paired-end/single reads for which both reads map unambiguously one gene, removing multi-hits. According to these rules, around 96% of PE reads were associated to a gene, 2% PE reads unmapped and 2% of PE reads with multi-hits were removed.

For differential analysis, we discarded genes, which did not have at least 1 read after a count per million (CPM) normalization, in at least one half of the samples. The library sizes were normalized using the method TMM and the count distribution was modeled with a negative binomial generalized linear model where the harvest date was taken into account. Dispersion was estimated by the edgeR method (McCarthy et al., 2012) in the statistical software 'R' (R Core team, 2015). The p-values were adjusted by the Benjamini-Hochberg procedure to control FDR and a gene was declared differentially expressed if its adjusted p-value was lower than 0.05.

Transcriptome analysis

BAR (http://www.bar.utoronto.ca/) and its Classification SuperViewer Tool (Provart et Zhu, 2003), based on the GO functional classifications, was used to calculate normed frequencies of the classes, bootstrap standard deviations, and P values. AgriGO (Du et al., 2010) was also used for detailed analysis of GO term enrichment. Genes related to flowering time were extracted from the FLOR-ID interactive database (Bouché et al., 2015) and the ThaleMine data mining of the ARAPORT project (https://apps.araport.org/thalemine/). For the analysis of the transcription factors we used the PlantTFDB 4.0 (Plant Transcription Factor Database, http://planttfdb.cbi.pku.edu.cn/). The genes related to chromatin were identified as in Chupeau et al (2013). Hierarchical clustering was performed using the Multiple Experiment Viewer tool (MeV), the Pearson correlation metric and average linkage clustering as linkage method (Saeed et al., 2003).

Venn diagrams were constructed using the tool VENNY 2.1 (http://bioinfogp.cnb.csic.es/tools/venny/index.html).

Long non-coding RNAs (lncRNAs) analysis

We built a non-redundant dataset (IJPB_lncDS) of 14 621 putative long non-coding RNAs (lncRNAs) sequences based on the assembling of lincRNAs or lncRNAs datasets resulting from previous studies (Supplemental figure 1a). In case of an overlap of contiguous transcription units (TUs) annotated as lncRNAs, the largest TU was assembled, named lncRNA_merge_AIx and conserved. We kept the strand information of the transcripts, when available. After removal of the redundant TUs, we established three fasta files of putative lncRNAs: one with 5 055 putative TUs on positive strand, another one with 4 851 putative TUs on negative strand and the last one of 4 715 TUs with no strand information.

We then remapped all reads against IJPB_lncDB using Bowtie version 2. The abundance of each TU was calculated by a local script using Sam2 tool and we counted only reads mapped unambiguously, removing multi-hits. Despite the 96% of the paired-end reads mapped to the TAIR10 genome, the mean mapping percentage to the lncRNA dataset was only 0.78% (Supplemental figure 1b). To establish the differentially expressed lncTUs we used GLM edger without or with filter using either Bonferroni or BH corrections.

Acknowledgements

We thank Bruno Letarnec and Hervé Ferry for plant care in the greenhouses. We thank Rurika Oka for the feedback on the cluster analysis. S.D.P was supported by a PhD fellowship provided by the European Commission Seventh Framework-People-2012-ITN Project EpiTRAITS (Epigenetic regulation of economically important plant traits, no-316965). Swammerdam Institute for Life Sciences, University of Amsterdam supported S.D.P with a short-term fellowship. The funding provided by the ITN EpiTRAITS and INRA is gratefully acknowledged. The IJPB benefits from the support of the LabEx Saclay Plant Sciences-SPS (ANR-10-LABX-0040-SPS).

Supporting Information

a)

Data set	Number	Reference
A	36	Liu et al., 2012
B	469	Di et al., 2014
C	995	Di et al., 2014
D	278	Liu et al., 2012
E	36	Liu et al., 2012
F	32	Liu et al., 2012
G	61	Liu et al., 2012
H	6480	Liu et al., 2012
I	5049	NONCODEv4
J	4396	Di et al., 2014
K	98	FLAGdb++

b)

Replicate	Paired reads	% mapping reads	% multihits removed reads	% counted pairs
T0 BR1	45 542 220	0.69	6.14	0.58
T0 BR2	48 165 370	0.67	6.17	0.56
T0 BR3	42 134 256	0.70	6.48	0.59
T2 BR1	44 506 108	0.78	6.21	0.64
T2 BR2	47 126 174	0.78	6.60	0.66
T2 BR3	45 078 232	0.79	6.18	0.65
T3 BR1	44 073 307	0.76	6.19	0.64
T3 BR2	44 189 464	0.82	7.33	0.69
T3 BR3	41 052 667	0.77	6.17	0.65
T5 BR1	41 046 783	0.83	6.11	0.69
T5 BR2	43 207 137	0.83	6.55	0.70
T5 BR3	44 543 187	0.81	6.13	0.68
Min	41 046 783	0.67	6.11	0.56
Max	48 165 370	0.83	7.33	0.70
Median	44 347 786	0.78	6.19	0.65

Supplemental figure 1: Long non-coding RNAs (lncRNAs) analysis.
a) Composition of the IJPB_lncDS data set and associated references of the databases used.
b) LncRNAs statistics with generated and mapped reads in each biological replicate
.

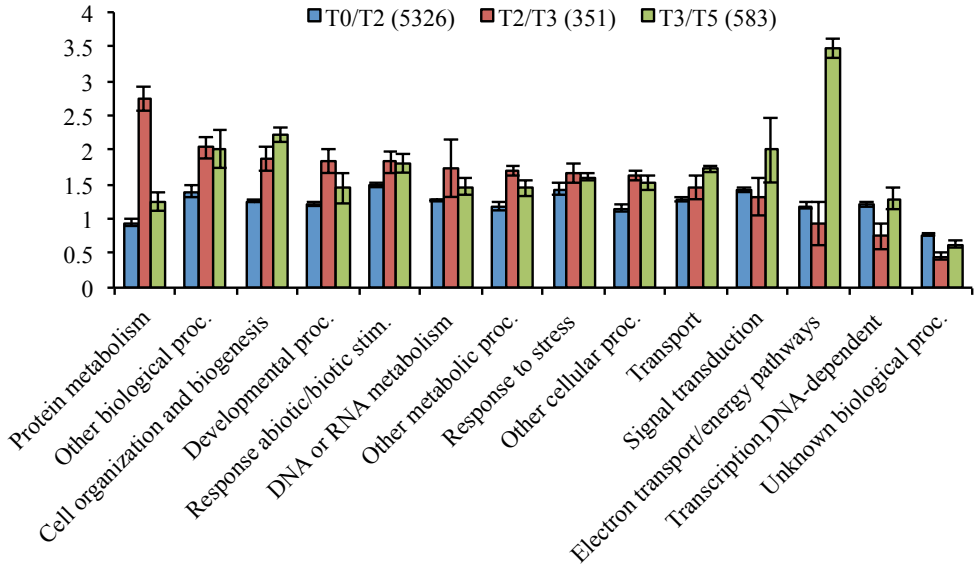

Supplemental figure 2: GO term enrichments within the specific T0/T2, T2/T3 and T3/T5 DEGs sets using BAR SuperViewer tool.

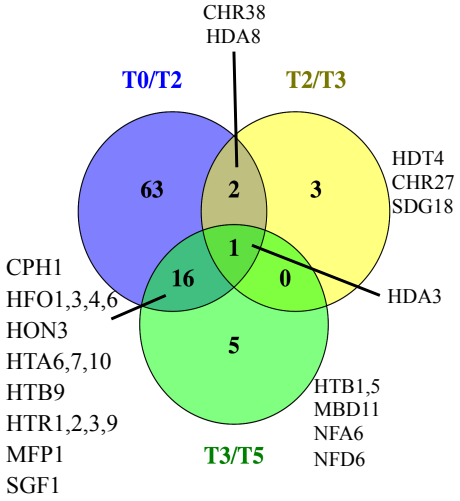

Supplemental figure 3: Venn diagram highlighting the chromatin-associated genes in the three comparisons.

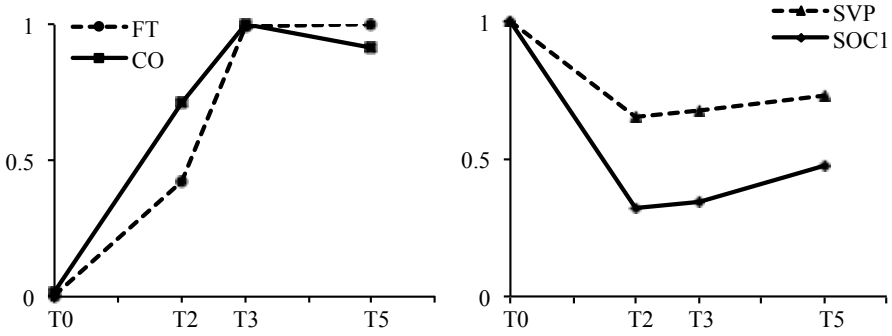

Supplemental figure 4: Expression profiles of flowering-time genes. The maximum normalization of the counted reads was used to obtain the expression values.

Library	Total paired reads	Overall alignment rate
T0 BR1	45 542 220	98.97
T0 BR2	48 165 370	99.23
T0 BR3	42 134 256	99.20
T2 BR1	44 506 108	99.03
T2 BR2	47 126 174	99.08
T2 BR3	45 078 232	99.09
T3 BR1	44 073 307	99.12
T3 BR2	44 189 464	98.78
T3 BR3	41 052 667	99.15
T5 BR1	41 046 783	99.07
T5 BR2	43 207 137	99.04
T5 BR3	44 543 187	99.08

Supplemental table 1: RNA-seq statistics with generated and mapped reads in each biological replicate.

.

Gene ID	Symbol	Name	Function	T0/T2 log2Fold Change	T2/T3 log2Fold Change	T3/T5 log2Fold Change
Giberellin (GA) associated genes						
AT5G56300	GAMT2	GA METHYLTRANSFERASE 2	GA metabolism		0.79	
AT1G80340	GA3OX2	GA 3-OXIDASE 2	GA9 to bioactive GA4 tranformation	2.80	0.62	
AT1G30040	GA2OX2	GA 2-OXIDASE	GA4 catabolism	0.90		
AT1G66350	RGL1	RGA-like 1	GRAS TF, Negative regulator of GA responses	1.54		
AT3G03450	RGL2	RGA-like 2	GRAS TF, Negative regulator of GA responses	1.05		
AT1G74670	GASA6	GA-STIMULATED ARABIDOPSIS 6	GA-regulated family protein	0.57		-1.28
AT4G32980	ATH1	homeobox protein	TF, regulating GA biosynthesis	0.31		
AT3G63010	GID1B	GA INSENSITIVE DWARF1A	GA receptor			0.67
AT3G05120	GID1A	GA INSENSITIVE DWARF1A	GA receptor	-0.47		
AT5G27320	GID1C	GA INSENSITIVE DWARF1C	GA receptor	-0.91		
AT1G79460	GA2/KS1	ENT-KAURENE SYNTHASE	GA biosynthesis	-1.50		0.47
AT1G15550	GA3OX1	GA 3-OXIDASE 1	GA biosynthesis	-1.15	-1.01	
AT4G25420	GA20OX1	GA 20-OXIDASE 1	GA biosynthesis	-1.24		
AT1G78440	ATGA2OX1	GA 2-beta-DIOXYGENASE	GA metabolism	-4.38		
AT1G22690	AT1G22690	Unknown	GA-regulated family protein	-1.23		-0.87
AT5G14920	GASA14	GA-STIMULATED IN ARABIDOPSIS 14	GA-regulated family protein			-0.71
Cytokinin (CK) associated genes						
AT5G06300	LOG7	LONELY GUY 7	cytokinin biosynthesis	0.90		1.11
AT5G11950	LOG8	LONELY GUY 8	cytokinin biosynthesis	0.67		
AT5G20040	IPT9	tRNA ISOPENTENYLTRANSFERASE9	cytokinin biosynthesis	-0.71		
AT4G29740	CKX4	CYTOKININ OXIDASE 4	cytokinin catabolism	-0.89		
AT3G63440	CKX6	CYTOKININ OXIDASE/DEHYDROGENASE 6	cytokinin catabolism			-0.66
AT5G21482	CKX7	CYTOKININ OXIDASE 7	cytokinin catabolism	1.05		
AT1G26210	SOFL1	SOB FIVE-LIKE 1	regulator of cytokinin levels	0.70		-1.35
AT1G68870	SOFL2	SOB FIVE-LIKE 2	regulator of cytokinin levels	1.41		

Supplemental table 2: List of the differentially expressed gibberellin and cytokinin related genes.
Log2 (Fold-Change) is reported

Locus Up regualted in root and in T0/T2 transition	Function
ADP/ATP CARRIER 2 (AAC2)	ADP/ATP carrier 2
ALPHA-AMYLASE-LIKE 2 (AMY2)	Alpha-amylase-like 2
ASPARAGINE SYNTHETASE 2 (ASN2)	Asparagine synthetase 2
AT1G03820	E6-like protein
AT1G33260	Protein kinase superfamily protein
AT1G55210	Disease resistance-responsive (dirigent-like protein) family protein
AT1G58170	Disease resistance-responsive (dirigent-like protein) family protein
AT1G59740	Major facilitator superfamily protein
AT1G66620	Protein with RING/U-box and TRAF-like domain
AT1G67360	Rubber elongation factor protein (REF)
AT2G44670	Senescence-associated family protein (DUF581)
AT3G02910	AIG2-like (avirulence induced gene) family protein
AT3G13560	O-Glycosyl hydrolases family 17 protein
AT3G15650	Alpha/beta-Hydrolases superfamily protein
AT3G25290	Auxin-responsive family protein
AT3G62060	Pectinacetylesterase family protein
AT5G26790	Transmembrane protein
AT5G42860	Late embryogenesis abundant protein, group 2
AT5G48460	Actin binding Calponin homology (CH) domain-containing protein
AT5G51310	2-oxoglutarate (2OG) and Fe(II)-dependent oxygenase superfamily protein
AT5G59480	Haloacid dehalogenase-like hydrolase (HAD) superfamily protein
ATMPK13	Protein kinase superfamily protein
TREHALOSE-6-PHOSPHATE PHOSPHATASE A (TPPA)	Haloacid dehalogenase-like hydrolase (HAD) superfamily protein
BREAST CANCER ASSOCIATED RING 1 (BARD1)	Breast cancer associated RING 1
CHLORIDE CHANNEL B (CLC-B)	Chloride channel B
CHROMOMETHYLASE 3 (CMT3)	Chromomethylase 3
CELLULOSE SYNTHASE LIKE D5 (CSLD5)	Cellulose synthase-like D5
CYTOCHROME C-2 (CYTC-2)	Cytochrome c-2, electron carrier
DEHYDRATION RESPONSE ELEMENT-BINDING PROTEIN 26 (DREB26)	Integrase-type DNA-binding superfamily protein
EMBRYO DEFECTIVE 2813 (EMB2813)	DNA primase, large subunit family
EXORDIUM LIKE 5 (EXL5)	EXORDIUM like 5
FLAVIN-MONOOXYGENASE GLUCOSINOLATE S-OXYGENASE 3 (FMO GS-OX3)	Flavin-monooxygenase glucosinolate S-oxygenase 3
GLUCOSE-6-PHOSPHATE DEHYDROGENASE 3 (G6PD3)	Glucose-6-phosphate dehydrogenase 3
GATA TRANSCRIPTION FACTOR 15 (GATA15)	GATA transcription factor 15
GLUTATHIONE S-TRANSFERASE TAU 20 (GSTU20)	Glutathione S-transferase TAU 20
ELONGATED HYPOCOTYL 5 (HY5)	Basic-leucine zipper (bZIP) transcription factor family protein
2,3-BIPHOSPHOGLYCERATE-INDEPENDENT PHOSPHOGLYCERATE MUTASE 2 (iPGAM2)	Phosphoglycerate mutase, 2,3-bisphosphoglycerate-independent
RESPONSE TO LOW SULFUR 2 (LSU2)	Response to low sulfur 2
ENDO-BETA-MANNASE 7 (MAN7)	Glycosyl hydrolase superfamily protein
MITOGEN-ACTIVATED PROTEIN KINASE KINASE KINASE 14 (MAPKKK14)	Mitogen-activated protein kinase kinase kinase 14
MANNAN SYNTHESIS RELATED 1 (MSR1)	O-fucosyltransferase family protein
NICOTIANAMINE SYNTHASE 1 (NAS1)	Nicotianamine synthase 1
PDI-LIKE 2-2 (PDIL2-2)	PDI-like 2-2
PLASMODESMATA-LOCATED PROTEIN 2 (PDLP2)	Plasmodesmata-located protein 2
CITY PHOSPHATASE 1 (PFA-DSP1)	Phosphotyrosine protein phosphatases superfamily protein
PHOSPHOGLYCERATE/BISPHOSPHOGLYCERATE MUTASE (PGM)	Phosphoglycerate/bisphosphoglycerate mutase
PHOSPHOENOLPYRUVATE CARBOXYLASE 1 (PPC1)	Phosphoenolpyruvate carboxylase 1
ROOT FNR 1 (RFNR1)	Root FNR 1
ROOT FNR 2 (RFNR2)	Root FNR 2
SAH7	Pollen Ole e 1 allergen and extensin family protein
SERINE CARBOXYPEPTIDASE-LIKE 46 (scpl46)	Serine carboxypeptidase-like 46
TOUCH 2 (TCH2)	EF hand calcium-binding protein family

Supplemental table 3: List of genes upregulated both in root and leaves during the SD-LD developmental switch.

The upregulated genes in root were extracted from Bouché et al. (2012).

Cluster	Nr. of DEGs	Gene Symbols
C1	2	*CHR38, HDA8*
C2	2	*HDT1, NFA6*
C3	2	*HON3, MBD11*
C5	28	*DML2, HAG2, HDA5, HFO2, HTA5, HTB2, HTB4, HTR1, HTR3, SDG4, EMF1*
C6	18	*HAC5, HDA2, HON2, HON8, HTA12, HTB3*
C7	4	*CHR27, HDT4, NFD6, SDG18*
C8	34	*CMT3, HFO1, HFO3, HFO4, HFO5, HFO6, HFO7, HTA1, HTA10, HTA11, HTA13, HTA2, HTA6, HTA7, HTA8, HTB1, HTB10, HTB11, HTB5, HTB6, HTB9, HTR12, HTR2, HTR3, HTR9, MET1, ULT1*

Supplemental table 4: Deregulated chromatin-associated genes in the nine clusters.
The number of DEGs and a selection of CA-DEGs are given for each cluster.

References

Argyros, R.D., Mathews, D.E., Chiang, Y.-H., Palmer, C.M., Thibault, D.M., Etheridge, N., Argyros, D.A., Mason, M.G., Kieber, J.J., and Schaller, G.E. (2008). Type B response regulators of Arabidopsis play key roles in cytokinin signaling and plant development. Plant Cell **20**: 2102–16.

Bernier, G. (2013). My favourite flowering image: the role of cytokinin as a flowering signal. J. Exp. Bot. **64**: 5795–5799.

Bernier, G. and Périlleux, C. (2005). A physiological overview of the genetics of flowering time control. Plant Biotechnol. J. **3**: 3–16.

Bouché, F., Aloia, M.D., Tocquin, P., Lobet, G., Detry, N., and Périlleux, C. (2016). Integrating roots into a whole plant network of flowering time genes in Arabidopsis thaliana. Nat. Publ. Gr.: 1–12.

Bouché, F., Lobet, G., Tocquin, P., and Périlleux, C. (2015). FLOR-ID: an interactive database of flowering-time gene networks in Arabidopsis thaliana. Nucleic Acids Res. **44**: gkv1054.

Bratzel, F. and Turck, F. (2015). Molecular memories in the regulation of seasonal flowering: from competence to cessation. Genome Biol. **16**: 192.

Carrio-Seguı, A., Romero, P., Sanz, A., and Penarrubia, L. (2016). Interaction between ABA signaling and copper homeostasis in Arabidopsis thaliana. Plant Cell Physiol. **57**: 1568–1582.

Castellano, M. del M., Boniotti, M.B., Caro, E., Schnittger, A., and Gutierrez, C. (2004). DNA replication licensing affects cell proliferation or endoreplication in a cell type-specific manner. Plant Cell **16**: 2380–93.

Chen, Y.-Y., Wang, Y., Shin, L.-J., Wu, J.-F., Shanmugam, V., Tsednee, M., Lo, J.-C., Chen, C.-C., Wu, S.-H., and Yeh, K.-C. (2013). Iron is involved in the maintenance of circadian period length in Arabidopsis. Plant Physiol. **161**: 1409–20.

Chupeau, M.-C., Granier, F., Pichon, O., Renou, J.-P., Gaudin, V., and Chupeau, Y. (2013). Characterization of the early events leading to totipotency in an Arabidopsis protoplast liquid culture by temporal transcript profiling. Plant Cell **25**: 2444–63.

Corbesier, L., Gadisseur, I., Silvestre, G., Jacqmard, A., and Bernier, G. (1996). Design in Arabidopsis thaliana of a synchronous system of floral induction by one long day. Plant J. **9**: 947–952.

Corbesier, L., Lejeune, P., and Bernier, G. (1998). The role of carbohydrates in the induction of flowering in Arabidopsis thaliana: Comparison between the wild type and a starchless mutant. Planta **206**: 131–137.

Costanzo, E., Trehin, C., and Vandenbussche, M. (2014). The role of WOX genes in flower development. Ann. Bot. **114**: 1545–1553.

Dewitte, W., Riou-Khamlichi, C., Scofield, S., Healy, J.M.S., Jacqmard, A., Kilby, N.J., and Murray, J.A.H. (2003). Altered Cell Cycle Distribution, Hyperplasia, and Inhibited Differentiation in Arabidopsis Caused by the D-Type Cyclin CYCD3. Plant Cell Online **15**: 79–92.

Fornara, F., de Montaigu, A., and Coupland, G. (2010). SnapShot: Control of flowering in arabidopsis. Cell **141**: 3–5.

Girin, T., Lejay, L., Wirth, J., Widiez, T., Palenchar, P.M., Nazoa, P., Touraine, B., Gojon, A., and Lepetit, M. (2007). Identification of a 150 bp cis-acting element of the AtNRT2.1 promoter involved in the regulation of gene expression by the N and C status of the plant. Plant, Cell Environ. **30**: 1366–1380.

Hauser, B.A., He, J.Q., Park, S.O., and Gasser, C.S. (2000). TSO1 is a novel protein that modulates cytokinesis and cell expansion in Arabidopsis. Development **127**: 2219–2226.

Haydon, M.J., Mielczarek, O., Robertson, F.C., Hubbard, K.E., and Webb, A.A.R. (2013). Photosynthetic entrainment of the Arabidopsis thaliana circadian clock. Nature **502**: 689–92.

Hecker, A., Brand, L.H., Peter, S., Simoncello, N., Kilian, J., Harter, K., Gaudin, V., and Wanke, D. (2015). The Arabidopsis GAGA-Binding Factor BASIC PENTACYSTEINE6 Recruits the POLYCOMB-REPRESSIVE COMPLEX1 Component LIKE HETEROCHROMATIN PROTEIN1 to GAGA DNA Motifs. Plant Physiol. **168**: 1013–24.

Van Houtte, H., López-Galvis, L., Vandesteene, L., Beeckman, T., and Van Dijck, P. (2013). Redundant and non-redundant roles of the trehalose-6-phosphate phosphatases in leaf growth, root hair specification and energy-responses in Arabidopsis. Plant Signal. Behav. **8**: e23209.

Imai, K.K., Ohashi, Y., Tsuge, T., Yoshizumi, T., Matsui, M., Oka, A., and Aoyama, T. (2006). The A-type cyclin CYCA2;3 is a key regulator of ploidy levels in Arabidopsis endoreduplication. Plant Cell **18**: 382–396.

Kimura, Y., Aoki, S., Ando, E., Kitatsuji, A., Watanabe, A., Ohnishi, M., Takahashi, K., Inoue, S.I., Nakamichi, N., Tamada, Y., and Kinoshita, T. (2015). A flowering integrator, SOC1, Affects stomatal opening in arabidopsis thaliana. Plant Cell Physiol. **56**: 640–649.

King, R.W., Hisamatsu, T., Goldschmidt, E.E., and Blundell, C. (2008). The nature of floral signals in Arabidopsis. I. Photosynthesis and a far-red photoresponse independently regulate flowering by increasing expression of FLOWERING LOCUS T (FT). J. Exp. Bot. **59**: 3811–3820.

Lamesch, P. et al. (2012). The Arabidopsis Information Resource (TAIR): Improved gene annotation and new tools. Nucleic Acids Res. **40**.

Langmead, B. and Salzberg, S.L. (2012). Fast gapped-read alignment with Bowtie 2. Nat Methods **9**: 357–359.

Lee, H.O., Davidson, J.M., and Duronio, R.J. (2009). Endoreplication : polyploidy with purpose. Genes Dev. **23**: 2461–2477.

Li, L., Li, X., Liu, Y., and Liu, H. (2016). Flowering responses to light and temperature. Sci. China Life Sci. **59**: 403–408.

Long, T. a, Tsukagoshi, H., Busch, W., Lahner, B., Salt, D.E., and Benfey, P.N. (2010). The bHLH transcription factor POPEYE regulates response to iron deficiency in Arabidopsis roots. Plant Cell **22**: 2219–2236.

Lu, T., Dou, Y., and Zhang, C. (2013). Fuzzy clustering of CPP family in plants with evolution and interaction analyses. BMC Bioinformatics **14 Suppl 1**: S10.

McCarthy, D.J., Chen, Y., and Smyth, G.K. (2012). Differential expression analysis of multifactor RNA-Seq experiments with respect to biological variation. Nucleic Acids Res. **40**: 4288–4297.

McClung, C.R., Lou, P., Hermand, V., and Kim, J.A. (2016). The Importance of Ambient Temperature to Growth and the Induction of Flowering. Front. Plant Sci. **7**: 1–7.

Orr-weaver, T.L. (2016). When Bigger Is Better : The Role of Polyploidy in Organogenesis. **31**: 307–315.

Ortiz-Marchena, M.I., Albi, T., Lucas-Reina, E., Said, F.E., Romero-Campero, F.J., Cano, B., Ruiz, M.T., Romero, J.M., and Valverde, F. (2014). Photoperiodic control of carbon distribution during the floral transition in Arabidopsis. Plant Cell **26**: 565–84.

Ortiz-Marchena, M.I., Romero, J.M., and Valverde, F. (2015). Photoperiodic control of sugar release during the floral transition: What is the role of sugars in the florigenic signal? Plant Signal. Behav. **10**: e1017168.

R Core team (2015). R Core Team. R A Lang. Environ. Stat. Comput. R Found. Stat. Comput. , Vienna, Austria. ISBN 3-900051-07-0, URL http//www.R-project.org/. **55**: 275–286.

Ranftl, Q.L., Bastakis, E., Klermund, C., and Schwechheimer, C. (2016). LLM-domain containing B-GATA factors control different aspects of cytokinin-regulated development in Arabidopsis thaliana. Plant Physiol. **170**: pp.01556.2015.

Riboni, M., Galbiati, M., Tonelli, C., and Conti, L. (2013). GIGANTEA enables drought escape response via abscisic acid-dependent activation of the florigens and SUPPRESSOR OF OVEREXPRESSION OF CONSTANS. Plant Physiol. **162**: 1706–19.

Riboni, M., Robustelli Test, A., Galbiati, M., Tonelli, C., and Conti, L. (2014). Environmental stress and flowering time: The photoperiodic connection. Plant Signal. Behav. **9**: 1–5.

Saeed, A.I. et al. (2003). TM4: A free, open-source system for microarray data management and analysis. Biotechniques **34**: 374–378.

Schmid, M., Uhlenhaut, N.H., Godard, F., Demar, M., Bressan, R., Weigel, D., and Lohmann, J.U. (2003). Dissection of floral induction pathways using global expression analysis. Development **130**: 6001–6012.

Schnittger, A., Schobinger, U., Bouyer, D., Weinl, C., Stierhof, Y.-D., and Hulskamp, M. (2002). Ectopic D-type cyclin expression induces not only DNA replication but also cell division in Arabidopsis trichomes. Proc. Natl. Acad. Sci. U. S. A. **99**: 6410–6415.

Song, Y.H., Shim, J.S., Kinmonth-Schultz, H. a, and Imaizumi, T. (2015). Photoperiodic Flowering: Time Measurement Mechanisms in Leaves. Annu. Rev. Plant Biol. **66**: 441–464.

Srikanth, A. and Schmid, M. (2011). Regulation of flowering time: All roads lead to Rome. Cell. Mol. Life Sci. **68**: 2013–2037.

Torti, S., Fornara, F., Vincent, C., Andrés, F., Nordström, K., Göbel, U., Knoll, D., Schoof, H., and Coupland, G. (2012). Analysis of the Arabidopsis shoot meristem transcriptome during floral transition identifies distinct regulatory patterns and a leucine-rich repeat protein that promotes flowering. Plant Cell **24**: 444–62.

Verkest, A., Manes, C.L., Vercruysse, S., Maes, S., Van Der Schueren, E., Beeckman, T., Genschik, P., Kuiper, M., Inze, D., and De Veylder, L. (2005). The cyclin-dependent kinase inhibitor KRP2 controls the onset of the endoreduplication cycle during Arabidopsis leaf development through inhibition of mitotic CDKA;1 kinase complexes. Plant Cell **17**: 1723–1736.

Wahl, V., Ponnu, J., Schlereth, A., Arrivault, S., Langenecker, T., Franke, A., Feil, R., Lunn, J.E., Stitt, M., and Schmid, M. (2013a). Regulation of flowering by trehalose-6-phosphate signaling in Arabidopsis thaliana. Science (80-.). **339**: 704–707.

Wahl, V., Ponnu, J., Schlereth, A., Arrivault, S., Langenecker, T., Franke, A., Feil, R., Lunn, J.E., Stitt, M., and Schmid, M. (2013b). Regulation of Flowering by Trehalose-6-Phosphate Signaling in Arabidopsis thaliana. Science (80-.). **339**: 704–708.

Zhang, J., Vankova, R., Malbeck, J., Dobrev, P.I., Xu, Y., Chong, K., and Neff, M.M. (2009). AtSOFL1 and atSOFL2 act redundantly as positive modulators of the endogenous content of specific cytokinins in Arabidopsis. PLoS One **4**: 1–11.